Electric Vehicle Charge Optimization Including Effects of Lithium-Ion Battery Degradation

Anderson Hoke, Alexander Brissette, Dragan Maksimović
University of Colorado, Boulder
Anderson.Hoke@Colorado.edu

Annabelle Pratt
Intel Labs
Annabelle.Pratt@Intel.com

Kandler Smith
National Renewable Energy Laboratory
Kandler.Smith@NREL.gov

***Abstract*-This paper presents a method for minimizing the cost of electric vehicle (EV) charging given variable electricity costs while also accounting for estimated costs of battery degradation using a simplified lithium-ion battery lifetime model. The simple battery lifetime model, also developed and presented here, estimates both energy capacity fade and power fade due to temperature, state of charge profile, and daily depth of discharge. This model has been validated by comparison with a detailed model [6], which in turn has been validated through comparison to experimental data. The simple model runs quickly in a MATLAB script, allowing for iterative numerical minimization of charge cost. EV charge profiles optimized as described here show a compromise among four trends: charging during low-electricity cost intervals, charging slowly, charging towards the end of the available charge time, and suppression of vehicle-to-grid power exportation. Finally, simulations predict that batteries charged using optimized charging last longer than those charged using typical charging methods, potentially allowing smaller, cheaper batteries to meet vehicle lifetime requirements.**

I. INTRODUCTION

As electric vehicles (EVs) and plug-in hybrid electric vehicles (PHEVs) are commercialized, interest has grown in predicting the effect such vehicles will have on electric power system infrastructure, and in mitigating any negative effects [1, 2, 3]. A proposed method of reducing stresses on grid infrastructure due to EV charging is by encouraging vehicles to charge at off-peak times through time-of-use electricity pricing [2, 4]. For a vehicle to respond to price signals, some degree of intelligent charge control is required. Such charge control could, for example, be implemented as part of a vehicle or home energy management system, provided that the algorithms involved are not prohibitively complex for embedded processing. This paper presents a relatively simple method of charge power control that optimizes not just the cost of energy, but also the equivalent estimated cost of battery degradation, as shown conceptually in Fig. 1.

Accounting for battery degradation during charge optimization is important because lithium-ion (Li-ion) batteries represent a major component of vehicle cost [5]. Finding the minimum battery size that meets vehicle energy capacity[1] and power output requirements presents an opportunity to reduce vehicle cost significantly [6]. The temperatures at which a battery is charged and the state of charge (SOC) as a function of time have significant effects on battery life [6]. Therefore, an intelligent charge algorithm capable of estimating and minimizing these effects can potentially extend battery life. A vehicle equipped with a charge controller that minimizes the effects of charging on battery life can potentially be equipped with a smaller, less expensive battery while still meeting battery capacity and power requirements over a specified vehicle lifetime.

The question of PHEV charge profile optimization has been addressed in [7], where an electrochemistry-based battery model is used in a genetic algorithm to find a Pareto front of optimal energy cost and battery resistance growth. In contrast, the intelligent charge algorithm presented here minimizes the total cost of charging, defined as the cost of energy plus the equivalent cost of battery degradation. To facilitate iterative, numerical minimization of total cost, this paper presents a simple model for estimating the cost of battery degradation. To be clear, this model is not intended to advance the science of lithium-ion battery life estimation, but only to efficiently capture the dominant effects present in advanced battery lifetime models. The simple model presented here has been verified through comparison of its results to those of a detailed model developed at the National Renewable Energy Laboratory (NREL) for Li-ion batteries with nickel-cobalt-aluminum (NCA) cathode[2] and graphite

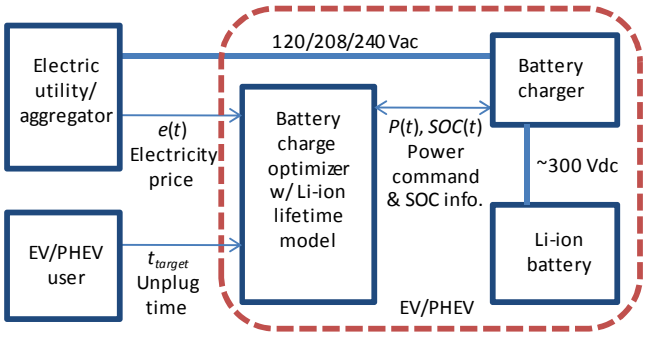

Fig. 1. EV/PHEV charge optimization schematic

[1] Battery energy capacity, defined as the maximum energy available from a fully charged battery, is often referred to herein simply as "capacity."

[2] The NCA Li-ion chemistry was chosen for degradation modeling due to the public availability of aging data for a wide variety of temperature and duty-cycle operating conditions. Cathode materials such as nickel-manganese-cobalt, manganese-spinel, and iron-phosphate may be preferred for present PHEV and EV designs due to their safety characteristics.

978-1-61284-247-9/11/$26.00 ©2011 IEEE

anode [6]. NREL's model has in turn been shown to agree well with experimental data [6]. It has not been established how well the NCA model will represent other Li-ion chemistries, but it is anticipated that other chemistries with similar degradation mechanisms could be modeled in a similar fashion after adjustment of model parameters.

II. Simple Battery Degradation Model

A. Overview

In order to simultaneously optimize battery life and energy cost, estimated equivalent costs of battery degradation are defined here in terms of battery lifetime reduction. The cost of battery degradation, c_{bd}, due to a charge cycle is defined as

$$c_{bd} = c_{bat} * \frac{\Delta L}{L} \quad (1)$$

Here c_{bat} is the cost to purchase the battery pack, ΔL is the lifetime degradation due to the charge cycle being evaluated per unit time, and L is the total battery lifetime if the charge cycle under evaluation were repeated until the battery's end of life (EOL). By minimizing c_{bd}, we are maximizing battery life. EOL for a vehicle drive battery is defined as the time when either the battery's energy capacity or its available power drops below a specified minimum. Typically, the EOL energy capacity Q_{EOL} is designed to be about 80% of the initial capacity Q_0 in order to provide the desired energy storage over the vehicle's design life at minimal cost: $Q_{EOL} = 0.8Q_0$ [8]. Battery power is typically oversized relative to the minimum design EOL power for economic reasons: additional power makes more energy accessible at low SOC without requiring addition of expensive active material [9]. To reflect this, EOL power is defined here as $P_{EOL} = 0.7P_0$, where P_0 is the initial maximum power, in agreement with [10].

Li-ion battery power fade P_{fade} is a result of internal resistance growth [6]. $P_{fade}(t)$ defined as $P_{max}(t)/P_0$, which is equal to $R_0/R(t)$, where P_{max} is as defined in [11], R_0 is the initial internal resistance, and $R(t)$ is the internal resistance at time t. This relationship is derived in Appendix A.

Over a daily battery cycle, significant factors that influence power fade and capacity fade are temperature $T(t)$, open circuit voltage $V_{OC}(t)$, and depth of discharge (DOD) [6]. The simple battery model proposed here makes two approximations: 1) Each of these effects is independent of the others, and 2) The effects themselves are independent of battery age. Approximation 1 allows the model to be simple enough to be evaluated quickly and allows it to be tuned to fit available data sets that often only consider one of the three factors. The degree of validity of this approximation is a complex question requiring further research. Approximation 2 allows the simple battery model to be time-invariant over battery life. As can be seen by comparing the slope of the curved relative power, $P(t)$, line in Fig. 2 to its average slope, this approximation is very good, but not perfect, over most of the battery lifetime. Finally, we note that V_{OC} maps directly to SOC.

Using these approximations to consider the effects of $T(t)$, $SOC(t)$, and DOD on capacity lifetime and power lifetime, we have that the cost of battery degradation is

$$c_{bd} = max\left((c_{Q,T} + c_{Q,SOC} + c_{Q,DOD}), (c_{P,T} + c_{P,SOC} + c_{P,DOD})\right)$$

where $c_{Q,T}$, $c_{Q,SOC}$, and $c_{Q,DOD}$ are the costs associated with capacity fade and $c_{P,T}$, $c_{P,SOC}$, and $c_{P,DOD}$ are the costs associated with power fade due to temperature, SOC, and DOD, respectively. The battery model presented here models all three capacity-related costs, as well as the cost of power fade due to temperature, $c_{P,T}$. The costs $c_{P,SOC}$ and $c_{P,DOD}$ are assumed to be negligible in comparison to the other costs based on [12] and hence are not modeled.

B. Temperature-related degradation: $c_{Q,T}$ and $c_{P,T}$

Estimates of the two temperature-related costs, $c_{Q,T}$ and $c_{P,T}$, are based on the Arrhenius relationship: $r = A * e^{-E/kT}$, where r is the rate of the reaction assumed to be behind the battery degradation, E is the activation energy of the reaction, k is Boltzmann's constant, T is battery temperature, and A is a proportionality constant [5]. Lifetime $L(T)$ is inversely proportional to r, so that $L(T) = ae^{b/T}$. Because temperature affects power fade and capacity fade differently, we define power lifetime $L_P(T) = a_P e^{b_P/T}$ and capacity lifetime $L_Q(T) = a_Q e^{b_Q/T}$. The a and b parameters in these equations are determined by fitting $L(T)$ to NREL model data as described in Section III.

It is anticipated that it will be useful in the future to adjust model parameters to fit physical data, updated models, and models of other Li-ion cathode chemistries. For this purpose a script has been developed to automatically tune the a and b parameters of $L(T)$ to fit three data points. The three data points can come from experimental data or from a detailed model such as NREL's. Details of the tuning process are described in Appendix B.

The temperature change produced by a given charge profile is approximated as a linear function of charge power so that $T(P) = T_{amb} + R_{th} * |P|$, where R_{th} is the thermal resistance of the battery pack (including any active cooling if present) and T_{amb} is the ambient temperature. This implies the approximation that the battery is always in thermal equilibrium, which is valid to the extent that the battery system's thermal time constant is short compared to the time spent at each power setpoint.[3] The absolute value of P is used so that $T(P)$ is valid for both charging and vehicle-to-grid (V2G) power exportation. To correctly calculate $c_{P,T}$ and $c_{Q,T}$, one should only include battery degradation that could have been avoided had the battery been charged in the least harmful manner possible. When accounting only for temperature-related degradation, the least damage is done by a slow, constant power charge at the minimum power P_{min} required to fully charge the battery in the available time t_{max}. So, charging at P_{min} for time t_{max} serves as the baseline against which other charge profiles are evaluated. This reasoning leads to equation (2) shown at the top of the next page for $c_{P,T}$ and $c_{Q,T}$ (with derivation in Appendix C). In (2), the placeholder subscript x becomes P when evaluating $c_{P,T}$, and it becomes Q when evaluating $c_{Q,T}$. The constant 8,760 is the

[3] The simple model presented here operates on one-hour time intervals, much longer than typical battery system thermal time constants, so the approximation is justified.

$$c_{x,T} = c_{bat} \cdot \left(\underbrace{\int_{t_{ch}} \frac{1}{8760 \cdot L_x\left(T_{amb} + R_{th} \cdot |P(t)|\right)} dt}_{\Delta L/L \text{ due to charging}} + \underbrace{\frac{t_{max} - t_{ch}}{8760 \cdot L_x\left(T_{amb}\right)}}_{\substack{\Delta L/L \text{ while plugged in} \\ \text{but not charging}}} - \underbrace{\frac{t_{max}}{8760 \cdot L_x\left(P_{min} \cdot R_{th} + T_{amb}\right)}}_{\substack{\text{Baseline } \Delta L/L \text{ that would be} \\ \text{expended by slow charging}}} \right) \quad (2)$$

number of hours in a year, and $\Delta L/L$ is battery life expended as a fraction of total lifetime, as defined previously.

C. *SOC-related degradation:* $c_{Q,SOC}$

The cost $c_{Q,SOC}$, which accounts for capacity fade attributable to $SOC(t)$, is calculated using a linear fit formula based on 15-year capacity versus average SOC data from [8]. The linear fit parameters have been tuned to fit more recent NREL model data points. We use the approximation of time-invariance explained above and the further approximation that, when accounting only for SOC-related degradation, a time period during which the SOC varies around an average of SOC_{avg} has the same effect on battery life as simply staying at SOC_{avg} for the same time period. The accuracy of this approximation varies by situation, but the approximation is necessary to arrive at a simple model that does not require high time-resolution SOC data. The following linear fit equation is derived from the data in [8] for the cost of one hour during which the average SOC is SOC_{avg}:

$$c_{Q,SOC} = c_{bat} \cdot \frac{m \cdot SOC_{avg} - d}{CF_{max} \cdot 15 \cdot 8760} \quad (3)$$

Here CF_{max} is the capacity fade at EOL, which we have taken above to be 100% - Q_{EOL}/Q_0 = 20%. The states of charge in question are presumed be limited by the vehicle's battery protection controls to a manufacturer-specified range, e.g., 30% < SOC < 90% [13].

D. *Depth of discharge degradation:* $c_{Q,DOD}$

The cost $c_{Q,DOD}$ accounts for capacity fade resulting from daily SOC swing ΔSOC, defined as the maximum daily SOC minus the minimum, also referred to as DOD. Effects of low amplitude, high frequency cycling, as would occur when a V2G-capable vehicle provides an ancillary service such as frequency regulation, are not captured in $c_{Q,DOD}$. (This type of cycling does result in temperature changes, so temperature-related degradation due to ancillary services is captured in $c_{Q,T}$ and $c_{P,T}$ if the model uses sufficient time resolution.) The calculation of $c_{Q,DOD}$ used here is based on data from [14] showing the effects of ΔSOC on battery lifetime in cycles, N:

$$N(\Delta SOC) = \left(\frac{\Delta SOC}{145.71} \right)^{-1/0.6844}$$

We make the approximation that n cycles at a given ΔSOC have the same effect as n cycles whose average SOC swing is equal to ΔSOC. It is difficult to determine the degree of validity of this approximation from the available data, but again the approximation is necessary to facilitate a simple model.

To estimate the cost associated with a cycle at ΔSOC_i, we employ the concept of *energy throughput* [15]. We define E_{TL} as the lifetime energy throughput (a function of ΔSOC_{avg}), $E_{T,used}$ as the total change in the remaining energy throughput due to a cycle, and $E_{T,base}$ as the minimum energy throughput required to recharge the battery. The cost $c_{Q,DOD}$ is then

$$c_{Q,DOD} = c_{bat} \cdot \left(E_{T,used} - E_{T,base}\right) / E_{TL} \quad (4)$$

Details on the calculation of each energy throughput are included in Appendix D.

III. Model Tuning and Verification

Despite the approximations made in estimating battery lifetime, the model can be quickly tuned so that its results agree well with NREL's model, which has been shown in [6] to agree well with physical data.

A. *Tuning* $c_{P,T}$

The cost of power degradation due to temperature, $c_{P,T}$, is tuned and verified by adjusting model parameters to fit data points from NREL's model. NREL's model takes as input the time history of battery current, voltage, SOC, and temperature. The time history spans one round-trip battery cycle, typically lasting 24 hours[4]. The 24-hour cycle is repeated over a simulation period of 10 years and battery state-of-life (SOL) parameters are calculated at specified times as shown in Fig. 2. The SOL parameters include relative capacity and relative internal resistance growth, which can be translated into relative power as described in Appendix A. The time when relative power crosses 0.7 is the power lifetime, L_P, in years, as indicated in Fig. 2. Recalling that $\Delta L/L$, the normalized lifetime lost per day, is the metric used to compute equivalent cost, we calculate the average $\Delta L/L$ per day that would result in a power lifetime L_P using

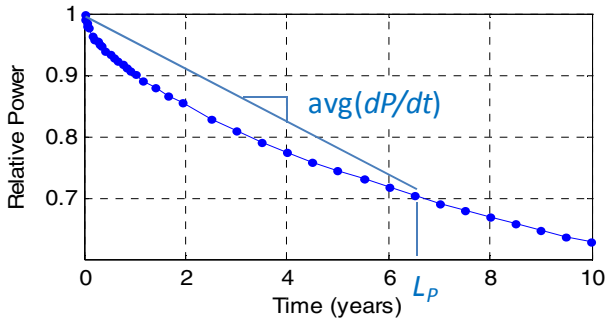

Fig. 2. Finding power lifetime L_P from NREL's model.

[4] A nominal discharge cycle profile must also be assumed in NREL's model. We select a slow, constant power discharge rather than a typical driving discharge profile so that the effects of discharging can be de-emphasized in order to evaluate various charge profiles.

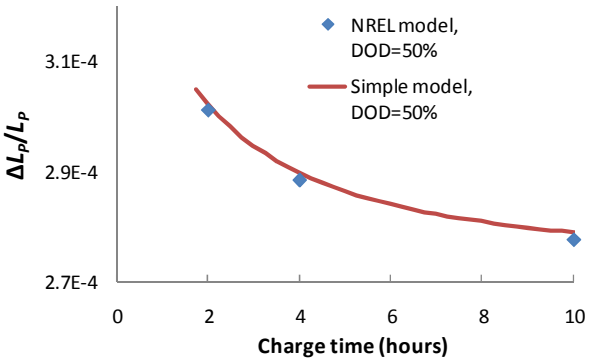

Fig. 3. Comparison of relative lifetime lost $\Delta L/L$ as estimated by NREL's model and by the simple model presented here, for power lifetime, DOD=50%.

$\Delta L/L = 1/(365L_P)$. In this manner, data points can be produced from NREL's model for comparison to $\Delta L/L$ values from the simple model as done in Fig. 3 for DOD = 50% and Q = 30 kWh. For comparison purposes, Fig. 3 assumes a maximum charge time of 12 hours and constant charge power. Charge times less than 2 hours correspond to charge powers over 6.6 kW (the maximum for Level 2 charging [13]) and hence are not shown.

Note that the good agreement between the two models in Fig. 3 is only present at the specific DOD to which $L_P(T)$ has been tuned (in this case 50%). To address this, $L_P(T)$ has been tuned at each 10% DOD interval, as shown in Fig. 4. The agreement between the simple model and NREL's model shown in Fig. 3 is representative of the agreement between the two models for each of the individually tuned L_P equations used to produce Fig. 4. For a given DOD, the $c_{P,T}$ calculations use the $L_P(T)$ equation for the nearest DOD to obtain good agreement with NREL's model for all DOD.

The cost of capacity fade due to temperature, $c_{Q,T}$, uses the same formula as $c_{P,T}$ and is tuned in the same manner as was just described. For this reason a detailed account of its tuning and verification is not included here.

B. *Tuning* $c_{Q,SOC}$

The cost of capacity fade due to $SOC(t)$, $c_{Q,SOC}$, was tuned by feeding into NREL's model various 24-hour battery data profiles with a constant, low temperature (6°C). This deemphasizes the effects of temperature degradation. Fig. 5 shows a plot of normalized lifetime lost $\Delta L/L$ versus average SOC for the various data sets. Note that the data form roughly a "V" shape; this is because degradation due to cycling (as accounted for by $c_{Q,DOD}$) is still present and is dominant at high DOD, which corresponds to low average SOC. To isolate the effects of average SOC, a linear fit was performed using only the data points above SOC_{avg} = 0.6, as shown by the dotted line and equation in Fig. 5. The linear fit determined the values of m and d in (3), completing the tuning of $c_{Q,SOC}$.

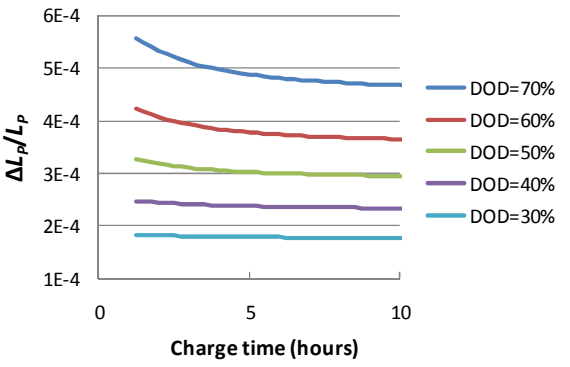

Fig. 4. Temperature-related relative lifetime lost, $\Delta L_P/L_P$, tuned to NREL's model at various DOD

The final cost component modeled here, the cost of capacity fade due to DOD, $c_{Q,DOD}$, is difficult to tune and verify because it turns out to be much smaller than $c_{Q,SOC}$ and $c_{Q,T}$. This is partially because NREL's model accounts for a DOD cycle corresponding to each slope change in $SOC(t)$, whereas the simple model considers only one DOD cycle per day. However, precisely because $c_{Q,DOD}$ is relatively insignificant, its accuracy will not have a major effect on model results. Further research is merited into modeling the effects of DOD cycles and into simplified modeling of battery degradation in general.

IV. Charge Optimization Algorithm

The total cost to charge an EV or PHEV, c_{tot}, is defined here as the sum of the cost of electrical energy, c_{kWh}, and the estimated cost of battery degradation, c_{bd}:

$$c_{tot} = c_{kWh} + c_{bd}$$

Mathematically, $c_{kWh} = \int_{t_{ch}} e(t) * P(t)dt$, where $e(t)$ is the electricity cost, $P(t)$ is the charge power, and t_{ch} is the time spent charging. Note that $P(t)$ may be negative for certain t, indicating V2G power exportation. The signal $e(t)$ is determined externally by a utility or microgrid controller. Also note that the electricity cost $e(t)$ can be constant or variable, and if variable, can be dynamic or static. In the case of a dynamic $e(t)$, each vehicle's charge profile is re-optimized upon a change in forecast $e(t)$.

The inputs to the charge optimization algorithm are electricity cost $e(t)$, battery energy capacity Q, initial SOC, plug-in time, and target time for full charge (where full charge is defined to be 90% SOC as is often done in practice to avoid accelerated battery degradation due to high V_{OC} at 100% SOC [11]).

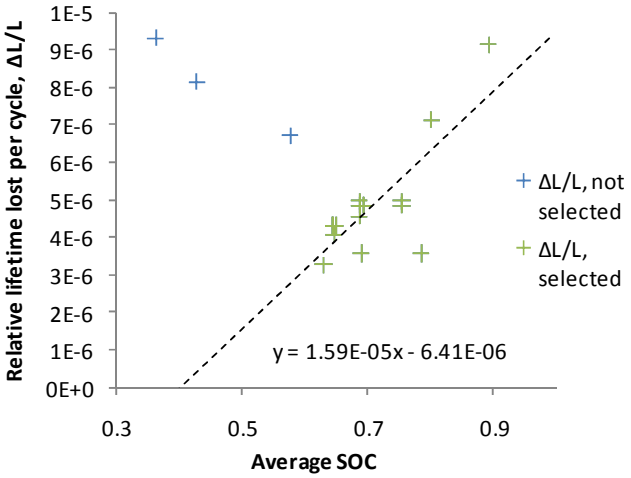

Fig. 5. Tuning SOC-related relative lifetime lost, $\Delta L/L$, to NREL model data

The output of the optimization algorithm is a charge profile that meets the constraints defined by the inputs and minimizes total cost c_{tot}. The charge optimization is implemented in MATLAB using the built-in nonlinear constrained optimization function fmincon(). To avoid local minima in c_{tot}, fmincon is seeded with various starting charge profiles and the result with the lowest cost c_{tot} is selected. The optimization runs in about 5 seconds per vehicle on a 2.8GHz Windows 7 machine. For comparison, NREL's accurate model runs in 5 to 10 seconds per iteration on the same machine; several thousand iterations would be required to find the minimum cost c_{tot}, so optimization using NREL's model directly would require several minutes. To implement a charge optimization algorithm in practice, it would be desirable to use more economical embedded computing, making the simplicity and speed of the model proposed here advantageous.

The charge optimization algorithm presented here optimizes charge power only. The charge current and voltage are to be managed separately by the vehicle charger.

V. Selected Optimization Results

A. Optimized charge profiles

The charge optimization algorithm was run simultaneously for three vehicles with different plug-in times, initial SOCs, and charge target times. Each vehicle had a 30-kWh battery pack with R_{th} = 0.002°C/W, and the ambient temperature was set to 25°C. The maximum charge and discharge powers were each 6.6 kW. Figs. 6 – 8 show optimized charge profiles under various pricing schemes. Colored arrows at the top of each figure indicate the user-supplied times when the vehicles plug-in in the evening and unplug in the morning. Note that the 24-hour clock begins at noon in these figures. The three EVs plug in with 35%, 30%, and 20% SOC, respectively.

In Fig. 6, the cost of power is a constant \$0.12/kWh. The three charge profiles all show a compromise between charging late in the available window and spreading of charge over time. The tendency to charge later is due to $c_{Q,SOC}$, which discourages spending time at high SOC (i.e., high V_{OC}). The spreading of charge over time is due to $c_{Q,T}$ and $c_{P,T}$, which discourage high power (i.e., high temperature) charging.

In Fig. 7, a simple two-level cost structure is used, such as might be implemented to encourage charging at off-peak times. The vehicles now avoid charging at powers higher than a few hundred watts during the high-cost interval. The two competing trends seen in Fig. 6 (spreading out charge and charging late in the available window) are present in Fig. 7 as well.

Fig. 8 uses a more complex pricing scheme such as might be used to encourage valley-filling of overnight power demand. The vehicles show a strong preference for charging in the lowest-cost interval. Note however that the vehicles do not charge at the maximum available power even during the short lowest-cost interval. This is done to avoid the high $c_{Q,T}$ and $c_{P,T}$ that come with high powers. Also note that no charging is performed during the highest cost interval.

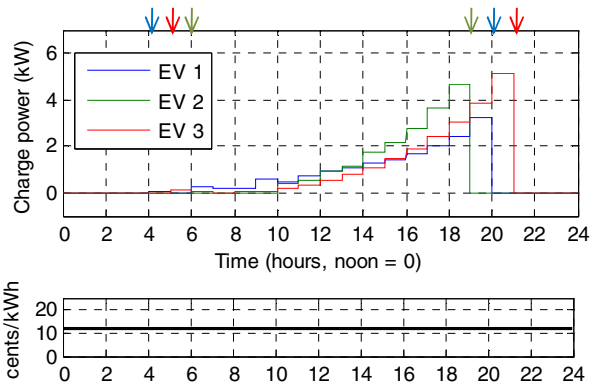

Fig. 6. Optimized charging of 3 EVs with constant cost of energy

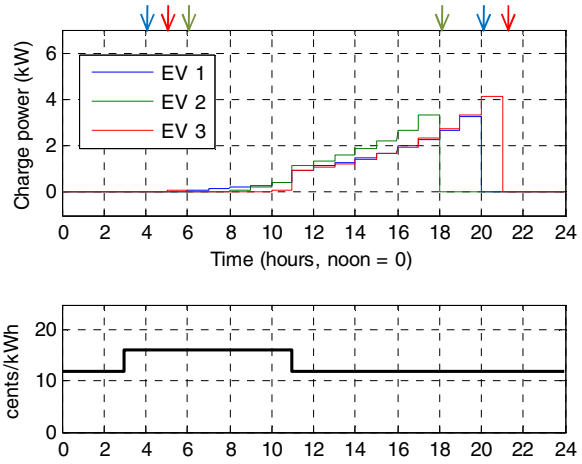

Fig. 7. Optimized charging of 3 EVs with simple two-level cost of energy

Vehicles in Figs. 6 – 8 were free to perform V2G power exportation, but the optimization chose not to do so because the potential profit from power arbitrage was outweighed by the cost of battery degradation. If the peak power price is increased significantly to about \$0.50/kWh, V2G becomes profitable for the simulation parameters in Figure 7, but at very low powers only. This is partially because any energy exported must subsequently be imported back, leading to additional temperature-related degradation. While this result

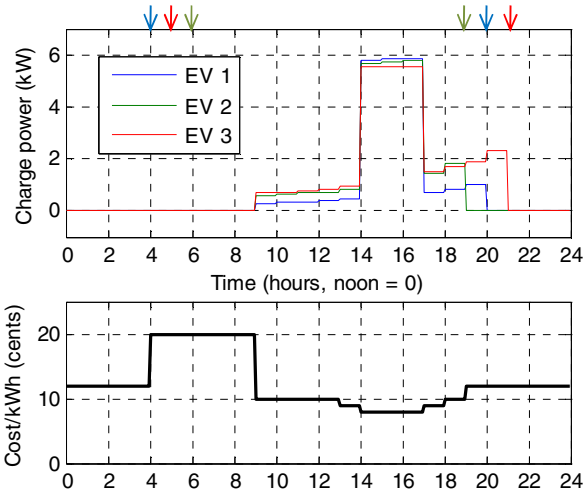

Fig. 8. Optimized charging of 3 EVs with multi-level cost of energy

indicates that a very high price differential is required to make V2G economical, it should be noted that low amplitude, high-frequency V2G associated with frequency regulation is not modeled here and may be economical at lower prices, especially if peak charge and discharge powers (and hence temperatures) are low.

Because the cost of battery degradation due to V2G is dominated by the temperature-related costs, effective thermal management should make V2G economical at lower power prices. This is demonstrated in Fig. 9, where R_{th} has been lowered by 80% to 0.0004°C/W. Initial SOCs for the three vehicles have been set at 50%, 80%, and 70%, respectively. All three vehicles export power at rates between 1 kW and 2 kW. Also note that V2G is performed as early as possible in the available window to maximize the amount of time spent at low SOC, reducing $c_{Q,SOC}$.

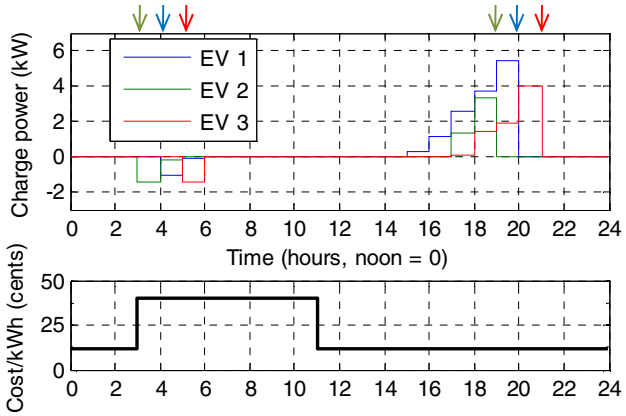

Fig. 9. Optimized charging of 3 EVs showing V2G operation

It is interesting to note that in simulations with R_{th} set one order of magnitude lower at $4*10^{-5}$°C/W (representing a nearly perfect and possibly impractical thermal management system), the vehicles begin to perform V2G even with constant energy price. In other words, the benefit of lowering SOC alone justifies power exportation in this hypothetical scenario.

B. *Battery lifetime comparisons*

To confirm that the charge optimization method presented here actually reduces battery degradation, the optimized charge profile for EV 2 in Fig. 6 was fed back into NREL's model to compute the estimated battery lifetime, assuming the charge cycle is repeated daily. The drive cycle was represented by an 8-hour, constant power discharge to de-emphasize driving effects. Fig. 10 shows battery lifetimes for this optimized charge profile along with battery lifetimes for various other charging schemes. Both energy capacity life and power life were computed for each charge profile; the actual battery life is the lesser of the two and is shown darker in Fig. 10. The charge schemes labeled "Charge on plug-in," "Late 6.6 kW charge," and "Delayed charge" all charge the battery at the maximum Level II charge rate of 6.6 kW. "Charge on plug-in" begins charging when the vehicle is first plugged in, "Delayed charge" begins charging at 12 a.m., and "Late 6.6 kW charge" was charged at the latest possible time. "Slow charge" spreads charging evenly over the entire available window, and "8 hour charge" spreads charging evenly over the final 8 hours. "Late fast charge" charges the

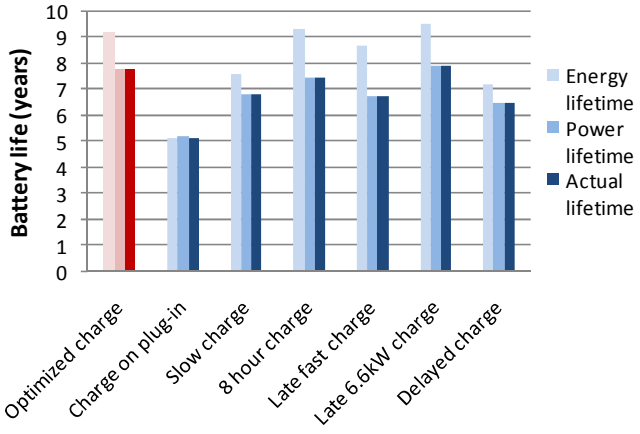

Fig. 10. Estimated battery life for various charge scenarios

vehicle entirely in the last hour, requiring 18 kW of power. The optimized charge results in longer battery life than all but the "Late 6.6 kW" scenario, which results in longer battery life by just 0.6%, well within the uncertainty of the models. Nevertheless, the fact that NREL's model predicts that a late, relatively high power charge results in a battery life similar to the optimized case suggests that the simple model underestimates $SOC(t)$-related degradation relative to temperature-related degradation. The estimated lifetime under optimized charging is between 4% and 50% longer than the lifetime under the other scenarios considered.[5]

The results presented here differ significantly from those of [7], the one previous paper to optimize both energy cost and battery life. In [7], the incentive to delay charge to avoid high V_{OC} is identified, just as here. However, because the effect of temperature rise is not considered, [7] does not identify the simultaneous incentive to spread out charge nor does it fully capture the effects of V2G. The results of [7] do address both charge voltage and charge current. Because the present paper addresses only charge power on a time scale of minutes to hours, a lower level of charge control is needed to provide real-time voltage and current settings. Also, [7] optimizes over both the driving interval and the charge interval, whereas here we assume no knowledge of the drive interval. Finally, [7] does not translate battery degradation into an equivalent cost and hence identifies a large family of charge profiles rather than a single actionable profile.

VI. Conclusions

This paper presents a method for minimizing the cost of EV charging given variable electricity costs while also accounting for estimated costs of battery degradation using a newly developed, simplified Li-ion battery lifetime model. It has been shown that batteries charged using the proposed optimized charge power algorithm, which includes simple modeling of the costs of battery degradation, are predicted to live longer than batteries charged using other charging

[5] Note that power lifetime is shorter than capacity lifetime in most cases modeled in Fig 10. This implies that allowing battery power to fade to 70% of its initial value has not been sufficient to obtain a battery that is oversized for power. In future work, $L_P(T)$ should be re-tuned to allow for more power fade.

methods. This result has been confirmed using NREL's more accurate battery lifetime model, which in turn has been shown to agree with physical data.

The charge optimization presented here results in charge profiles that follow four competing trends: 1) charging during low electricity price intervals, 2) spreading of charge over time to avoid high temperatures, 3) charging near the end of the available charge time, and 4) suppression of high-power V2G except during times of high electricity price. Trends 1 and 2 should tend to reduce stress on utility transformers by encouraging low-power charging at off-peak times. The possibility that trend 3 could overload transformers in the early morning can be mitigated by intelligent management of electricity price schedules, as demonstrated conceptually in Fig. 8.

As battery lifetime models are refined, it is expected that the details of charge optimization results presented here will change but that the general principle of balancing the estimated costs of battery degradation against the cost of electricity will remain useful. In addition, it is expected that the four trends identified will persist, although the relative weight given to each will likely change.

ACKNOWLEDGEMENTS

The authors Hoke, Brissette and Maksimović gratefully acknowledge funding provided by Intel Labs to CU-Boulder.

NREL's battery life model was developed under funding from the U.S. Department of Energy (DOE) Office of Vehicle Technologies Energy Storage Program with support of DOE program managers David Howell and Brian Cunningham.

APPENDICES

A. Finding power fade from internal resistance.

The relationship $P_{fade}(t) = R_0/R(t)$ is derived as follows: The maximum discharge power is defined as $P_{max\_disch} = V_{min}*(V_{OC\_disch}-V_{min})/R_{disch}$, and the maximum charge/ regeneration power is $P_{max\_ch} = V_{max}*(V_{max}-V_{OC\_ch})/R_{ch}$ [11]. V_{min} and V_{max} are the manufacturer's minimum and maximum operating battery voltages, R is the internal resistance, the subscripts *disch* and *ch* refer to discharging and charging, and V_{OC} is the battery open circuit voltage, which is a function of SOC. Making the approximation that $V_{OC}(SOC)$ does not change with age, for both charge and discharge we have equations of the form $P_{max} = V_a*V_b/R(t)$ where V_a and V_b are constant with respect to time. Therefore $P_{fade}(t) = P_{max}(t)/P_0 = R_0/R(t)$, where R_0 is the initial internal resistance. So, despite the unusual definition of P_{max} [11], we can still conclude that discharge power fade is inversely proportional to discharge resistance, and that charge power fade is inversely proportional to charging resistance.

B. Autotuning L(T)

A MATLAB script has been developed to tune the a and b parameters in $L(T) = ae^{b/T}$ using the method described here. For fixed DOD, thermal resistance R_{th}, battery capacity Q_0, and length of plug-in interval t_{max}, we define the function $\Lambda(t_{ch}) = \Delta L(t_{ch})/L(t_{ch})$ to represent the relative lifetime lost due to charging in time $t_{ch}<t_{max}$. Note that t_{ch} determines average charge power P, and P in turn determines average charging temperature T, so $\Lambda(t_{ch})$ determines $\Lambda(T)$. We now define $\Lambda_S(t_{ch})$ to be the relative lifetime lost as calculated by the simple degradation model and $\Lambda_{NREL}(t_{ch})$ to be the relative lifetime lost as calculated by NREL's model. Experimentally, it was determined that aligning Λ_S with Λ_{NREL} for t_{ch} = 2, 4, and 10 hours leads to a good match between the two models over the entire range of typical EV charge times. Hence the tuning process begins by generating (Λ_{NREL}, t_{ch}) data points for t_{ch} = 2, 4 and 10. Recalling the equation for Λ_S, we have:

$$\Lambda_S = \frac{\Delta L}{L} = \frac{t_{ch}}{8760 * L(T)} + \frac{t_{max} - t_{ch}}{8760 * L(T_{amb})}$$

$$= \frac{1}{8760a}\left(\frac{t_{ch}}{e^{b/T}} + \frac{t_{max} - t_{ch}}{e^{b/T_{amb}}}\right)$$

We define $\Lambda_{2\_4} = \Lambda(2) - \Lambda(4)$ and $\Lambda_{4\_10} = \Lambda(4) - \Lambda(10)$, where Λ represents either Λ_S or Λ_{NREL} (we are setting the two Λ functions equal). Further defining $H = \frac{\Lambda_{4\_10}}{\Lambda_{2\_4}}$, we note that H is independent of a; it is a function only of b and t_{ch}, the time spent charging. Hence we can solve numerically for b using the three known (Λ_{NREL}, t_{ch}) data points. Two values of b exist for most H, one for which $d\Lambda/dt_{ch} > 0$ and one for which $d\Lambda/dt_{ch} < 0$. The correct b can be selected based on the knowledge that $d\Lambda/dt_{ch} > 0$ is physically unrealistic: higher temperatures do not lead to less battery degradation. Once b is known, a can be found so that $\Lambda_S = \Lambda_{NREL}$ for any of the three (Λ_{NREL}, t_{ch}) data points.

C. Estimating temperature-related degradation

Using the approximation that battery degradation is time-invariant as mentioned in Section II, we can conclude that one hour at temperature T uses up a fractional lifetime $\Delta L/L = 1/(365*24*L(T))$, where $L(T) = ae^{b/T}$ is the total number of years the battery would last at that temperature. From (1) therefore, the cost per hour is $c = c_{bat}/(8760*L(T))$, and the cost of an arbitrary temperature profile is $c_{bat}\int \frac{1}{8760*L(T)}dt$. When comparing the costs of different possible charge profiles for a given maximum charge time t_{max}, we include: 1) the integral of cost over the time spent charging, t, and 2) the cost of sitting at ambient temperature for any remaining time. And 3) we subtract the minimum cost to charge in the most battery-friendly manner, as described in Section II. Thus the three terms in equation (2) are derived.

D. Energy throughput calculations

A battery's lifetime energy throughput for a given average ΔSOC is $E_{TL} = N(\Delta SOC)*\Delta SOC*Q$, where $N(\Delta SOC) = \left(\frac{\Delta SOC}{145.71}\right)^{-1/0.6844}$ as defined in Section II, and Q is the battery energy capacity, taken to be constant here. When a battery is discharged by ΔSOC_{base}, we can define a baseline energy throughput $E_{T,base} = N(\Delta SOC_{base})* \Delta SOC_{base}*Q$. A cycle with an SOC swing of ΔSOC_i changes the average ΔSOC slightly to $\Delta SOC_{avg,i}$ and also uses up an energy throughput of ΔSOC_i*Q. The energy throughput used by the cycle is then $E_{T,used} = N(\Delta SOC_{avg,i})*\Delta SOC_{avg,i}*Q+ \Delta SOC_i*Q$. These three

energy throughput values can be used in equation (4) to calculate $c_{Q,DOD}$.

REFERENCES

[1] S. Rajagopalan, "Power Electronics in Renewable Energy and Electric Transportation from a Utility Perspective," *IEEE Energy Conversion Congress and Expo 2010*, Atlanta, GA, Sept. 2010.

[2] P. Denholm and W. Short, "An Evaluation of Utility System Impacts and Benefits of Optimally Dispatched Plug-In Hybrid Electric Vehicles," NREL Technical Report NREL/TP-620-40293, National Renewable Energy Laboratory: Golden, CO, Oct. 2006.

[3] J. Tomic and W. Kempton, "Using Fleets of Electric-Drive Vehicles for Grid Support," *Journal of Power Sources*, vol. 168, issue 2, pp. 459–468, Jun. 2007.

[4] S. Shengnan et al., "Impact of TOU rates on Distribution Load Shapes in a Smart Grid with PHEV Penetration," *Transmission and Distribution Conference and Exposition, 2010 IEEE PES*, Apr. 2010.

[5] J. Belt, "Long Term Combined Cycle and Calendar Life Testing," *214th Electrochemical Society Meeting*, Honolulu, HI, INL/CON-08-14920, Oct. 2008.

[6] K. Smith, T. Markel, G.-H. Kim, and A. Pesaran, "Design of Electric Drive Vehicles for Long Life and Low Cost," *IEEE 2010 Workshop on Accelerated Stress Testing & Reliability,* Denver, CO, NREL/PR-540-48933, Oct. 2010.

[7] S. Bashash, S.J. Moura, J.C. Forman, and H.K. Fathy, "Plug-In Hybrid Electric Vehicle Charge Pattern Optimization for Energy Cost And Battery Longevity," *Journal of Power Sources*, vol. 196, pp, 541-549, Jul. 2010.

[8] T. Markel, K. Smith, and A. Pesaran, "Improving Petroleum Displacement Potential of PHEVS Using Enhanced Charging Scenarios," *EVS-24 International Battery, Hybrid and Fuel Cell Electric Vehicle Symposium*, Stravanger, Norway, NREL/CP-540-45730, May 2009.

[9] K. Smith, "Battery Life Trade-Off Studies," NREL Fiscal Year 2010 Annual Progress Report.

[10] A.A. Pesaran, T. Markel, H.S. Tataria, and D. Howell, "Battery Requirements for Plug-In Hybrid Electric Vehicles – Analysis and Rationale," *EVS-23 International Electric Vehicle Symposium,* Anaheim, CA, NREL/CP-540-42240, Dec. 2007.

[11] *Battery Test Manual for Plug-In Hybrid Electric Vehicles*, Rev. 2, Idaho National Laboratory, Idaho Falls, ID, INL/EXT-07-12536, Dec. 2010.

[12] J.C. Hall, A. Schoen, A. Powers, P. Liu, K Kirby, "Resistance Growth in Lithium Ion Satellite Cells," *208th Electrochemical Society Meeting*, Los Angeles, CA, Oct. 2005.

[13] S. Clark, "Optimization of Battery Thermal Management, and Impact on Life," *EV Battery Tech USA*, Troy, Michigan, Sept. 2010.

[14] C. Rosenkranz, "Deep-Cycle Batteries for Plug-In Hybrid Application," *EVS-20 International Electric Vehicle Symposium and Exhibition*, Long Beach, CA, Nov. 2003.

[15] V. Marano, S. Oroni, Y Guezennec, G. Rizzoni, N. Madella, "Lithium-ion Batteries Life Estimation for Plug-in Hybrid Electric Vehicles," *IEEE Vehicle Power and Propulsion Conference 2009*, Dearborn, MI, Sept. 2009.